Monte Carlo study of cluster-diameter distribution: An observable to estimate correlation lengths

Wolfhard Janke and Stefan Kappler
Institut für Physik, Johannes Gutenberg-Universität Mainz, Staudinger Weg 7, 55099 Mainz, Germany
(Received 17 July 1996)

We report numerical simulations of two-dimensional q-state Potts models with emphasis on a new quantity for the computation of spatial correlation lengths. This quantity is the cluster-diameter distribution function $G^{\mathrm{diam}}(x)$, which measures the distribution of the diameter of stochastically defined cluster. Theoretically it is predicted to fall off exponentially for large diameter x, $G^{\mathrm{diam}} \propto \exp(-x/\xi)$, where ξ is the correlation length as usually defined through the large-distance behavior of two-point correlation functions. The results of our extensive Monte Carlo study in the disordered phase of the models with $q=10$, 15, and 20 on large square lattices of size 300×300, 120×120, and 80×80, respectively, clearly confirm the theoretically predicted behavior. Moreover, using this observable we are able to verify an exact formula for the correlation length $\xi_d(\beta_t)$ in the disordered phase at the first-order transition point β_t with an accuracy of about 1%–2% for all considered values of q. This is a considerable improvement over estimates derived from the large-distance behavior of standard (projected) two-point correlation functions, which are also discussed for comparison. [S1063-651X(97)11907-9]

PACS number(s): 05.50.+q, 75.10.Hk, 64.60.Cn, 11.15.Ha

I. INTRODUCTION

The physics of phase transitions is essentially governed by the behavior of the spatial correlation length ξ. While in some problems, e.g., at a continuous phase transition where ξ diverges, it is often sufficient to know the qualitative behavior, there are also many applications which rely on quantitative estimates of ξ. This applies in particular to the finite-size scaling behavior near a first-order phase transition [1] where ξ stays finite and sets the length scale above which asymptotic considerations should apply [2]. Since analytical predictions are scarce it is therefore of great practical importance to develop refined numerical methods for reliable computations of correlation lengths.

In order to evaluate the accuracy of a newly proposed method one should apply it first to models where analytical predictions are available. The best known example is the two-dimensional (2D) Ising model where ξ is exactly known at all temperatures [3]. But already the generalization to the 2D q-state Potts model [4] complicates the theoretical analysis considerably, and much less is known analytically. It was therefore a great success when a few years ago at least the correlation length $\xi_d(\beta_t)$ in the disordered phase *at* the first-order transition point β_t for $q \geqslant 5$ could be calculated exactly [5–7]. Apart from heuristic arguments, no analytical predictions are available for the correlation length $\xi_o(\beta_t)$ in the ordered phase, and previous numerical simulations [8–10] turned out to be difficult to interpret. This was the physical motivation to start a project [11,12] with the goal to clarify conflicting conjectures for the ratio ξ_o/ξ_d at β_t. The idea was, of course, to test the employed numerical methods first for the exactly known correlation length in the disordered phase [11] and then to proceed to the so-far-unexplored ordered phase [12].

One often employed way to extract correlation lengths is to study the exponential decay of two-point correlation functions in the asymptotic limit of large distances. While this method works perfectly for the 2D Ising model, for $\xi_d(\beta_t)$ of the 2D q-state Potts models with $q=10$, 15, and 20 we experienced quite nasty systematic deviations from the exact answer by about 10%–20% [11]. The deviations could be traced back to the unexpected importance of higher-order excitations, but even though the Monte Carlo simulations were performed on quite large lattices and with a high statistics of about 50 000–100 000 uncorrelated measurements, least-squares fits with sufficiently many correction terms turned out to be too unstable to predict reliable numbers.

A way out of this problem is to search for a different estimator of ξ which is less affected by correction terms. A systematic search is certainly very difficult, but one possible candidate was recently suggested in analytical work [13] making extensive use of the Fortuin-Kasteleyn cluster representation [14] of the Potts model. In Ref. [13] it was shown that the distribution of the cluster diameter, $G^{\mathrm{diam}}(x)$, decays exponentially for large diameter x, and that the decay constant is identical to the inverse correlation length (as defined from the decay of the two-point correlation function). This prompted us to investigate if the cluster-diameter distribution function is better suited for a numerical determination of the correlation length. In the following we report high-statistics Monte Carlo simulations of the models with $q=10$, 15, and 20, focusing on the properties of the new observable. As the main result it turns out to be indeed very well suited in the disordered phase, allowing for the first time a confirmation of the analytical formula for $\xi_d(\beta_t)$ with an accuracy of about 1%–2%. Since we used larger lattices and considerably higher statistics than in our previous studies [11], we discuss for comparison also the newly obtained estimates for $\xi_d(\beta_t)$ from two different projections of the standard two-point correlation function.

The remainder of the paper is organized as follows. In Sec. II we first recall the definition of the model and some

exact results. We then discuss the simulation techniques and in particular describe the various estimators used to measure the correlation length. The results of our simulations are presented in Sec. III, and in Sec. IV we conclude with a brief summary of the main results and some final remarks.

II. MODEL AND OBSERVABLES

In our Monte Carlo simulations we used the standard definition of the Potts model partition function [4],

$$Z=\sum_{\{s_i\}} e^{-\beta E},\quad E=-\sum_{\langle ij\rangle}\delta_{s_i s_j},\quad s_i=1,\ldots,q, \tag{1}$$

where $\beta=J/k_BT$ is the inverse temperature in natural units, i denote the lattice sites of a square lattice, $\langle ij\rangle$ are nearest-neighbor pairs, $\delta_{s_i s_j}$ is the Kronecker delta symbol, and q is the number of states per spin. In all simulations we used periodic boundary conditions to minimize finite-size effects.

In the following we report results for the models with $q=10$, 15, and 20, employing lattices of size $V=L\times L$ with $L=300$, 120, and 80, respectively. All simulations were performed in the canonical ensemble at the infinite-volume first-order transition point $\beta_t=\ln(1+\sqrt{q})$, at which the ordered and disordered phase can coexist. In a Monte Carlo simulation, the system can be biased into one of the two phases by the choice of the initial spin configuration. To update the spins we used the Wolff single-cluster algorithm [15]. From a previous comparative study [11] we knew that in the disordered phase this algorithm clearly outperforms all other standard algorithms such as the Metropolis, heat-bath, and Swendsen-Wang multiple cluster [16] algorithms.

The lattice sizes were chosen such that, for each value of q, $L\approx 28\xi_d(\beta_t)$, with $\xi_d(\beta_t)=10.559\,519\ldots$, $4.180\,954\ldots$, and $2.695\,502\ldots$ for $q=10$, 15, and 20, respectively [5–7]. Starting from a completely random configuration of spins it is then extremely probable that the system will stay in the disordered phase for a sufficiently long time, allowing statistically meaningful measurements of quantities being characteristic for the pure disordered phase. More precisely, by recalling that the escape probability $\mathcal{P}$ is proportional to $\exp(-2\sigma_{od}L)$ and that in two dimensions the interface tension σ_{od} can be expressed in terms of the correlation length of the disordered phase [7], $\sigma_{od}=1/2\xi_d(\beta_t)$, one easily arrives at the order-of-magnitude estimate $\mathcal{P}\propto\exp[-L/\xi_d(\beta_t)]\approx\exp(-28)\approx 10^{-12}$. Finite-size corrections in the pure disordered phase are expected to be of the same order.

In this work we mainly focused on measurements of the probability distribution of the cluster diameter, $\mathrm{diam}C_{i_0}$, which, in general, is defined as the maximal extension of a cluster in any of the D coordinate directions of a hypercubic lattice; for an illustration see Fig. 1. The cluster-diameter distribution function $G^{\mathrm{diam}}(x)$ is then the probability

$$G^{\mathrm{diam}}(x)=\mu(\mathrm{diam}C_{i_0}=x) \tag{2}$$

that the cluster C_{i_0} connected to a lattice site i_0 has a given diameter x [13]. To increase the statistics we took advantage of the periodic boundary conditions and averaged $G^{\mathrm{diam}}(x)$ over all lattice sites i_0. In practice this amounts to recording a histogram $H^{\mathrm{diam}}(x)$, whose entries at $x=\mathrm{diam}C$ are incremented by the size or weight $|C|$ of each simulated cluster. If properly normalized, $H^{\mathrm{diam}}(x)$ is then an estimator of the probability distribution $G^{\mathrm{diam}}(x)$. As discussed in the Introduction the theoretically expected asymptotic behavior of $G^{\mathrm{diam}}(x)$ in the disordered phase is an exponential decay governed by the correlation length ξ_d [13],

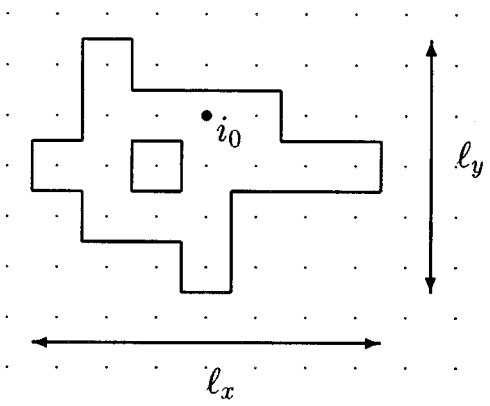

FIG. 1. Illustration of the definition of the cluster diameter $\mathrm{diam}C_{i_0}=\max\{\ell_x,\ell_y\}$.

$$G^{\mathrm{diam}}(x)=a\exp(-x/\xi_d)+\cdots. \tag{3}$$

By taking the logarithm of G^{diam} and performing linear two-parameter fits it is then straightforward to extract ξ_d.

For comparison we considered also in the new simulations the $k_y^{(n)}=2\pi n/L$ momentum projections $[i=(i_x,i_y)]$

$$g^{(n)}(i_x,j_x)=\frac{1}{L}\sum_{i_y,j_y}G(i,j)e^{ik_y^{(n)}(i_y-j_y)}, \tag{4}$$

with $n=0$ and 1 of the two-point correlation function

$$G(i,j)\equiv\left\langle \delta_{s_i s_j}-\frac{1}{q}\right\rangle. \tag{5}$$

For the measurements we actually decomposed the whole spin configuration into stochastic Swendsen-Wang (multiple) cluster and used the improved cluster estimator [17]

$$G(i,j)=\frac{q-1}{q}\langle\Theta(i,j)\rangle, \tag{6}$$

where $\Theta(i,j)=1$, if i and j belong to the same cluster, and $\Theta=0$ otherwise. In particular, for small average single-cluster sizes (cf. Table I), this procedure is more efficient than using directly the corresponding improved single-cluster estimator.

As discussed previously [11], to extract ξ_d from the large-distance behavior of Eq. (4), nonlinear four-parameter fits of the form

$$g^{(n)}(x)\equiv g^{(n)}(i_x,0)=a\,\cosh\left(\frac{L/2-x}{\xi_d^{(n)}}\right)+b\,\cosh\left(c\,\frac{L/2-x}{\xi_d^{(n)}}\right), \tag{7}$$

TABLE I. The average and maximum cluster size $\langle|C|\rangle$ and $|C|_{\max}$, the maximum cluster diameter (diam $C_{i_0})_{\max}$, the integrated autocorrelation time $\tau_{\mathrm{int},e}$ of the energy, the number of Monte Carlo update sweeps (MCS) in units of $\tau_{\mathrm{int},e}$, and the number of measurements N_{meas}.

$\beta=\beta_t$, disordered phase, single-cluster algorithm			
	$q=10$	$q=15$	$q=20$
	300×300	120×120	80×80
$\langle\|C\|\rangle_{\mathrm{SC}}$	38.093(17)	10.2254(11)	5.87776(75)
$\langle\|C\|\rangle_{\mathrm{SW}}$	2.726411(61)	2.117866(18)	1.854135(26)
$\|C\|_{\max}$	9353	1908	846
$(\mathrm{diam}\ C_{i_0})_{\max}$	197	73	51
$\tau_{\mathrm{int},e}$	≈59	≈18	≈25
MCS/$\tau_{\mathrm{int},e}$	600 000	9 000 000	4 200 000
N_{meas}	1 600 000	12 800 000	10 395 000

with

$$\xi_d \approx \xi_d^{(n)} / \sqrt{1-(2\pi n \xi_d^{(n)}/L)^2} \tag{8}$$

are necessary. Below we shall report results for the first two projections with $n=0$ and $n=1$. While the $n=0$ projection has been studied before on smaller lattices [11], the use of the $n=1$ projection in the disordered phase is actually also new. Originally this projection was applied in the ordered phase where it is essential for removing constant background terms caused by the nonzero magnetization [10,12]. Notice that for the large lattice sizes used in this study, $L\approx28\xi_d$, the difference in Eq. (8) between the fit parameter $\xi_d^{(n)}$ and ξ_d is only about 2.4%.

The computer code was implemented on a T3D parallel computer in a trivial way by running 64 independent simulations in parallel. This allowed us to generate the very high statistics compiled in Table I. Here we followed the usual convention and defined $V/\langle|C|\rangle_{\mathrm{SC}}$ single-cluster steps as one Monte Carlo update sweep (MCS), where $\langle|C|\rangle_{\mathrm{SC}}$ is the average cluster size, and rescaled the integrated autocorrelation time of the internal energy, $\tau_{\mathrm{int,e}}$, to this unit of time. Per $\tau_{\mathrm{int,e}}$ we performed about two measurements of the projected correlation functions. The size and diameter of the clusters were measured for each generated cluster. The statistical error bars are estimated from the fluctuations among the 64 independent copies by using the standard jackknife procedure [18]. The total running time of the simulations amounts to about 5 years of CPU time on a typical workstation.

III. RESULTS

In all simulations we monitored the time evolution of the energy and magnetization to convince ourselves that the system never escaped into the ordered phase. As a more quantitative measure we also computed energy and magnetization moments [19] which can be compared with exact [4,20] or series expansion results [21]. The average and maximum cluster sizes and the maximum cluster diameter found in the simulations are given in Table I. As a result of these tests we are convinced that, despite the very long run times, our results for ξ_d can be identified with the *pure* disordered phase correlation length.

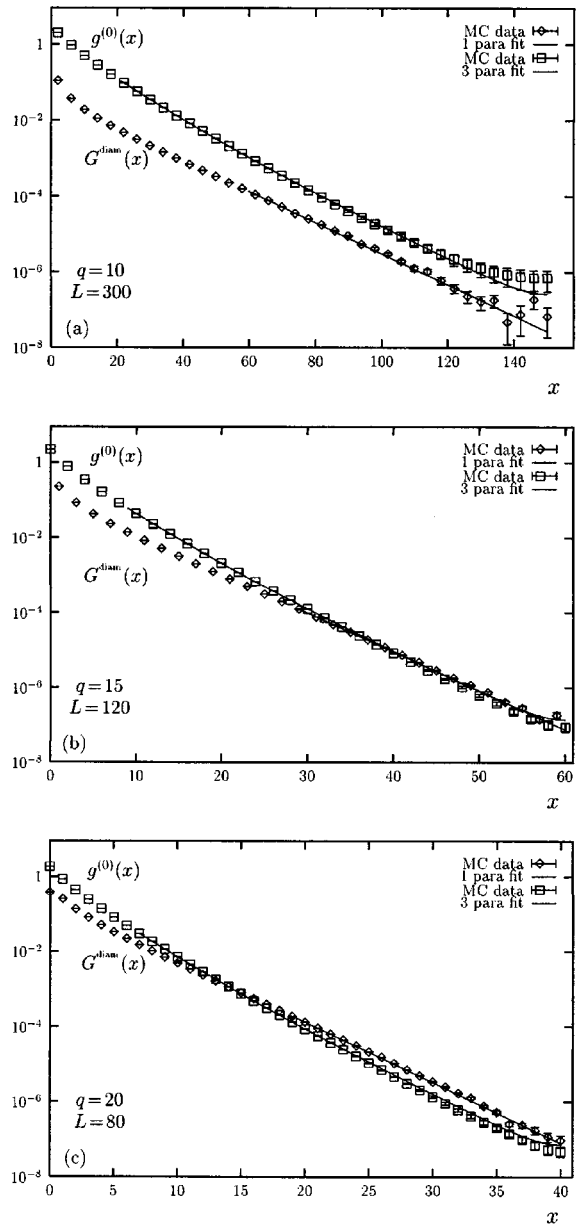

FIG. 2. Semilogarithmic plot of the cluster-diameter distribution $G^{\mathrm{diam}}(x)$ and the projected correlation function $g^{(0)}(x)$ for $q=10$, 15, and 20 at β_t in the disordered phase. For clarity some data points are omitted for $q=10$ and 15.

The data for $G^{\mathrm{diam}}(x)$ and $g^{(0)}(x)$ are shown for $q=10$, 15, and 20 in the semilogarithmic plots of Fig. 2. The solid lines are one- and three-parameter fits to the *Ansätze* (3) and (7), respectively, with ξ_d held fixed at its theoretical value ($=10.559\,519\ldots$, $4.180\,954\ldots$, and $2.695\,502\ldots$ for $q=10$, 15, and 20 [5–7]). Let us first concentrate on the new observable, the cluster-diameter probability distribution $G^{\mathrm{diam}}(x)$. At first sight the constrained one-parameter fit to G^{diam} looks less perfect than the constrained three-parameter fit to $g^{(0)}$, since the data points are more randomly scattered around the fit. The reason is that the correlations between the estimates at x and $x+\Delta x$ are much smaller for $G^{\mathrm{diam}}(x)$ than

TABLE II. Results for $\xi_d(\beta_t)$ from two-parameter fits (3) to $G^{\rm diam}(x)$ for different fit intervals $x_{\rm min}\cdots x_{\rm max}$, with $x_{\rm max}=130$, 50, and 40 for $q=10$, 15, and 20, respectively. Also shown are results of four-parameter fits to $g^{(0)}(x)$ and $g^{(1)}(x)$ according to the *Ansätze* (7), (8), with $x_{\rm max}=150$, 60, and 40 for $q=10$, 15, and 20, respectively.

Observable	$q=10$ 300×300		$q=15$ 120×120		$q=20$ 80×80	
exact	10.559519 . . .		4.180954 . . .		2.695502 . . .	
	$x_{\rm min}$	ξ_d	$x_{\rm min}$	ξ_d	$x_{\rm min}$	ξ_d
$G^{\rm diam}$	40	10.90(2)	20	4.297(4)	13	2.766(3)
	48	10.92(3)	23	4.286(5)	15	2.761(3)
	56	10.88(3)	26	4.267(8)	17	2.752(5)
	64	10.84(5)	29	4.26(2)	19	2.744(7)
	72	10.75(8)	32	4.25(2)	21	2.74(1)
	80	10.6(2)	35	4.27(3)	23	2.73(2)
	88	10.5(2)	38	4.25(4)	25	2.70(3)
	96	10.3(3)	40	4.23(6)	27	2.68(4)
$g^{(0)}(x)$	10	8.9(1)	5	3.56(2)	3	2.30(1)
	12	9.0(1)	6	3.60(2)	4	2.33(1)
	14	9.1(2)	7	3.63(2)	5	2.36(2)
	16	9.2(2)	8	3.66(3)	6	2.39(3)
	20	9.4(3)	9	3.70(4)	7	2.41(4)
	22	9.5(4)	10	3.73(5)	8	2.43(5)
	24	9.7(6)	11	3.76(6)	9	2.46(6)
$g^{(1)}(x)$	10	8.88(7)	5	3.55(1)	3	2.293(7)
	12	8.96(9)	6	3.59(2)	4	2.33(1)
	14	9.1(1)	7	3.62(2)	5	2.36(2)
	16	9.2(2)	8	3.65(3)	6	2.38(2)
	20	9.3(3)	9	3.69(3)	7	2.40(3)
	22	9.5(3)	10	3.72(4)	8	2.42(4)
	24	9.6(4)	11	3.75(5)	9	2.44(6)

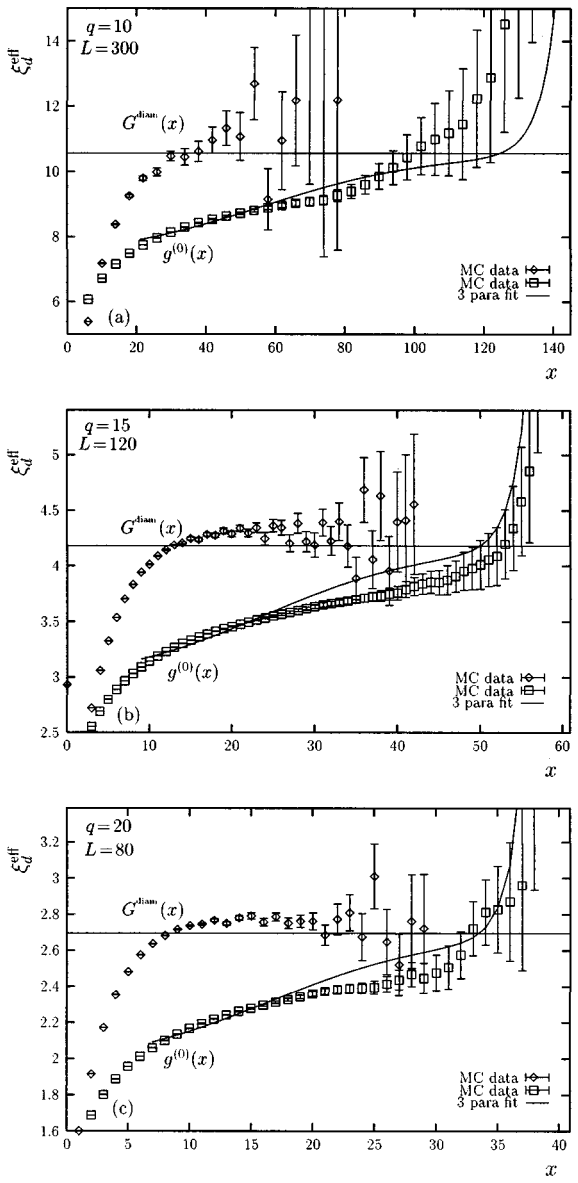

FIG. 3. Effective correlation lengths for $q=10$, 15, and 20 at β_t in the disordered phase derived from the correlation functions shown in Fig. 2.

for $g^{(0)}(x)$. This can be understood by noting that a cluster of diameter x_0 contributes only to the *one* estimate of $G^{\rm diam}(x)$ at $x=x_0$, but to *all* estimates of $g^{(0)}(x)$ with $x\leqslant x_0$ [recall the cluster estimator (6)].

The correlation-length estimates resulting from various unconstrained two-parameter fits to $G^{\rm diam}$ in intervals $x_{\rm min}\ldots x_{\rm max}$ with $x_{\rm max}=130$, 50, and 40 for $q=10$, 15, and 20, respectively, are collected in Table II. We see that the results are in very good agreement with the theoretically expected values, with only slight systematic deviations of about 1%–2%. Contrary to the results [11] obtained from $g^{(0)}(x)$ the fitted values tend now to be overestimates for small $x_{\rm min}$. This tendency becomes obvious in Fig. 3 where we show the effective correlation lengths

$$\xi_d^{\rm eff}(x)=1/\ln[C(x)/C(x+1)], \tag{9}$$

with $C=G^{\rm diam}$ or $g^{(0)}$. The $\xi_d^{\rm eff}(x)$ are just the inverse of the local slopes in Fig. 2. By recalling that neighboring values of $G^{\rm diam}$ are much less correlated than those of $g^{(0)}$, this explains the much larger error bars on the data for $\xi_d^{\rm eff}$ derived from $G^{\rm diam}$. Observe that the $\xi_d^{\rm eff}$ obtained from $G^{\rm diam}$ develop a much more pronounced plateau for $q=15$ and 20 than for $q=10$, before also here the statistical errors increase and the data start to fluctuate around the theoretically expected value. To conclude this subsection, by using the cluster-diameter probability distribution as an estimator for the correlation length, we succeeded to confirm the theoretical prediction for $\xi_d(\beta_t)$ at a 1%–2% level.

It would of course be unfair to compare the final estimates obtained from $G^{\rm diam}(x)$ of the present study with the results from $g^{(0)}(x)$ of previous work [11] which used smaller lattices and lower statistics. In the present study we have therefore analyzed again $g^{(0)}(x)$. Furthermore, we discuss for the first time also $g^{(1)}(x)$ in the disordered phase. In Fig. 2 we see that the constrained three-parameter fits to $g^{(0)}$ yield an excellent description of the falloff of $g^{(0)}(x)$ over more than four decades. Still, from an unconstrained four-parameter fit

over the same x range with ξ_d as a free parameter we obtain for, e.g., $q=10$ an about 10% smaller value of $\xi_d=9.5(4)$. This confirms our earlier observation in Ref. [11] that four-parameter fits to $g^{(0)}$ systematically underestimate ξ_d. This is demonstrated in more detail in Table II where we have collected the results of various fits in the intervals $x_{\min}\cdots x_{\max}=L/2$. For all three values of q we observe a clear tendency of increasing estimates for ξ_d with increasing $x_{\min}$. Still, the estimates in the last line for $g^{(0)}(x)$ are about 8%–10% below the theoretical values. This tendency is also clearly visible in the behavior of the $\xi_d^{\rm eff}(x)$ of $g^{(0)}$ shown in Fig. 3. Compared with Ref. [11] the linear lattice sizes of the present simulations are larger by a factor of 2 and the statistics is higher by more than one order of magnitude. This allowed us to include larger x values in the fits and, as expected, improved the estimates of ξ_d, in particular for $q=15$ and 20. This clearly indicates that by further increasing the statistics also the remaining discrepancies could be removed. We can therefore conclude that there is nothing wrong, in principle, in using the standard two-point correlation function to estimate ξ_d. Numerically, however, accurate estimates would require an enormous effort and would thus be a rather expensive enterprise.

In Table II we also give the results of unconstrained four-parameter fits of the form (7) to $g^{(1)}(x)$ where, by using Eq. (8), we have already converted $\xi_d^{(1)}$ to $\xi_d\approx 1.02\xi_d^{(1)}$. We see that the estimates from $g^{(0)}$ and $g^{(1)}$ are strongly correlated, so that in the disordered phase nothing is gained by studying also the higher momentum projections.

Further investigations of the cluster-diameter distribution in the disordered phase of the two-dimensional Ising ($q=2$) and three-state Potts models revealed, however, that the new observable is not always advantageous. Our results for the Ising model from a very long simulation of a 80×80 lattice with $\mathrm{MCS}/\tau_{\mathrm{int},e}\approx 12\,288\,000=N_{\rm meas}$ in the disordered phase at $\beta=0.703\,408\,88\approx 0.8\beta_c$ are shown in Fig. 4. For $\beta<\beta_c$ the exact expression for the 2D Ising model correlation length is $\xi_d=1/(\beta^\star-\beta)$ [3], where the dual inverse temperature $\beta^\star$ is given by $[\exp(\beta)-1]\times[\exp(\beta^\star)-1]=q=2$. We see that here the $\xi_d^{\rm eff}$ derived from $G^{\rm diam}$ clearly overshoot the exact value of $\xi_d=2.620\,290\,6\ldots$ before they slowly approach it from above. Notice that β was adjusted such that ξ_d agrees roughly with the value of the $q=20$ model at β_t. The $\xi_d^{\rm eff}$ of $g^{(0)}$, on the other hand, coincide with the exact value already for very small x, and a simple two-parameter fit of the form (7) with $b=c=0$ in the range $x=1,\ldots,40=L/2$ yields $\xi_d=2.620\,29(14)$, in perfect agreement with the exact result. A fit of $G^{\rm diam}$ according to Eq. (3) using only large x values in the interval $x=40,\ldots,56$ gives a considerably higher estimate of $\xi_d=2.89(8)$ which, despite its large error bar, is only barely compatible with the theoretical value. The deviation is still about 10%.

If we choose $\beta=0.789\,184\,7\approx 0.9\beta_c$ (the dual inverse temperature of $\beta^\star=0.98$), such that the exact correlation length is twice as large, $\xi_d=5.240\,581\,2\ldots$, we obtain qualitatively the same picture. This is shown in Fig. 5 for a simulation of a 160×160 lattice with $\mathrm{MCS}/\tau_{\mathrm{int},e}\approx 3\,200\,000=N_{\rm meas}$. Here the linear fit of the data for $g^{(0)}$ in the range $x=1,\ldots,80=L/2$ yields $\xi_d=5.2400(6)$, again in nice agreement with the exact value. A fit of $G^{\rm diam}$ in the interval $x=80,\ldots,100$ with $\xi_d=5.6(3)$, on the other hand, deviates again considerably by about 7%.

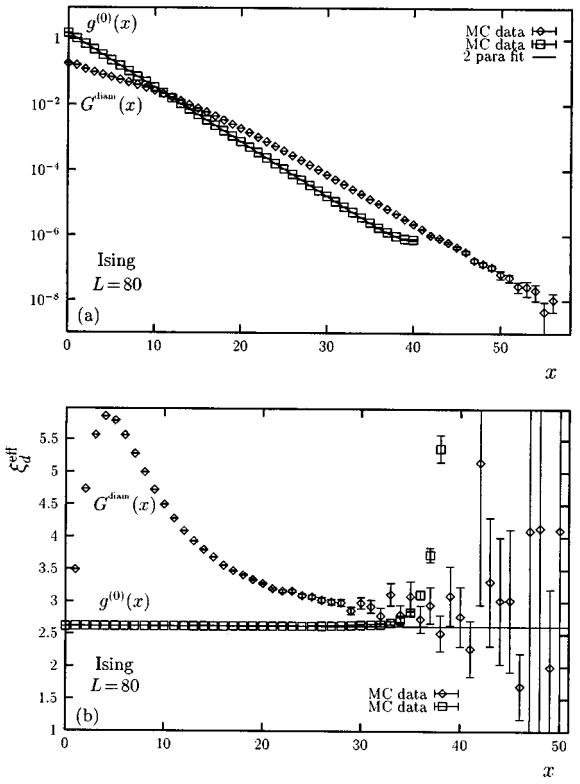

FIG. 4. Correlation functions (upper plot) and effective correlation lengths (lower plot) for the 2D Ising model at $\beta=0.703\,408\,88$. The horizontal line in (b) shows that exact value of $\xi_d=2.620\,290\,6\ldots$.

Finally we show in Fig. 6 our results for the two-dimensional three-state Potts model at $\beta=0.951\,795\,03\approx 0.95\beta_c$ (where $\beta^\star=1.06$). Here the lattice size is 160×160, $\mathrm{MCS}/\tau_{\mathrm{int},e}\approx 2\,285\,000$, and $N_{\rm meas}=3\,200\,000$. For small x we observe the influence of higher excitations in $g^{(0)}$ which, however, die out rapidly. Discarding therefore the smallest distances and choosing a fit interval of $x=7,\ldots,80=L/2$ we obtain an estimate of $\xi_d=5.838(2)$, which is shown as the horizontal line in the lower plot of Fig. 6. Here the cluster-diameter distribution $G^{\rm diam}$ is already slightly better behaved than for the two-dimensional Ising model, and a fit in the interval $x=80,\ldots,106$ gives a compatible value of $\xi_d=6.0(2)$, which now deviates only by about 2% from the result of $g^{(0)}$.

IV. DISCUSSION

Our numerical results clearly show that the cluster-diameter distribution $G^{\rm diam}(x)$ is very well suited to extract the correlation length $\xi_d(\beta_t)$ of two-dimensional q-state Potts models with relatively large values of q. While analyses of the standard (projected) two-point function are plaqued by large systematic errors, with the new observable we succeeded for the first time to reproduce the theoretically expected values at a 1%–2% level.

For small values of q, however, the standard correlation function gives much more reliable results. For reasons not well understood to date, the two quite different correlators

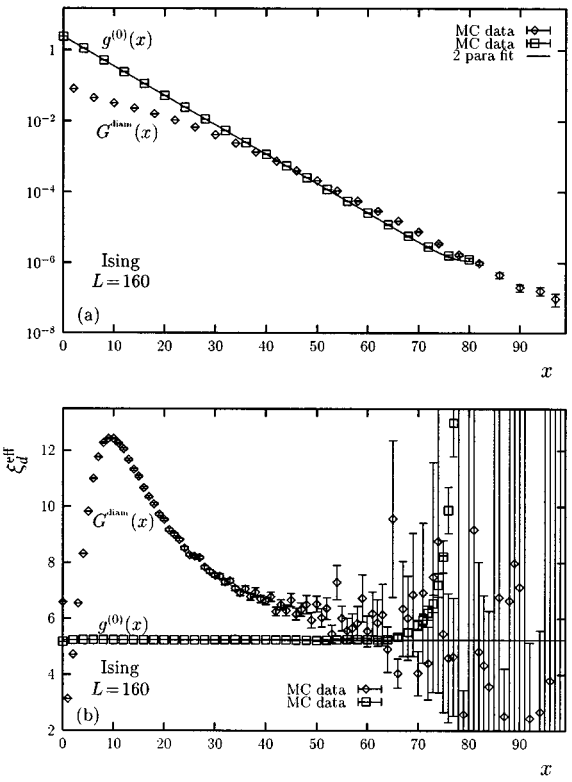

FIG. 5. Correlation functions (upper plot) and effective correlation lengths (lower plot) for the 2D Ising model at $\beta=0.789\,181\,47$. The horizontal line in (b) shows that exact value of $\xi_d=5.240\,581\,2\ldots$.

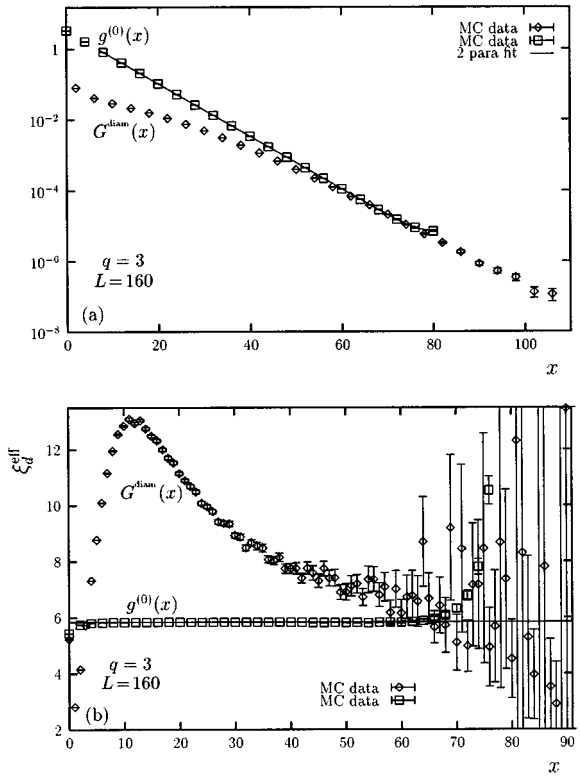

FIG. 6. Correlation functions (upper plot) and effective correlation lengths (lower plot) for the 2D three-state Potts model at $\beta=0.951\,795\,03$. The horizontal line in (b) shows our best numerical estimate of $\xi_d=5.838(2)$.

thus seem to behave complementary to each other.

Also for the three-dimensional q-state Potts models with $q=3$, 4, and 5, which undergo a first-order phase transition already for $q\geqslant 3$, our results [22] for $G^{\rm diam}$ and $g^{(0)}$ in the disordered phase at the transition point β_t as well as the corresponding effective correlation lengths look qualitatively as for the 2D Ising model in Fig. 4. Also in these cases we found that $g^{(0)}$ gives much more reliable estimates of ξ_d. This suggests that the behavior of $G^{\rm diam}$ does depend crucially on the value of q, but certainly not on the fact that the two-dimensional Potts models with $q=10$, 15, and 20 were studied at their first-order transition point β_t. The details of the 3D study will be published elsewhere [22].

ACKNOWLEDGMENTS

W.J. thanks the DFG for financial support and S.K. gratefully acknowledges support by the Graduiertenkolleg ''Physik and Chemie supramolekularer Systeme.'' Work supported by computer Grant Nos. hkf001 of HLRZ Jülich and bvpf03 of Norddeutscher Vektorrechnerverbund (NVV) Berlin-Hannover-Kiel.

[1] *Dynamics of First Order Phase Transitions*, edited by H.J. Herrmann, W. Janke, and F. Karsch (World Scientific, Singapore, 1992); K. Binder, Rep. Prog. Phys. **50**, 783 (1987); J.D. Gunton, M.S. Miguel, and P.S. Sahni, in *Phase Transitions and Critical Phenomena*, edited by C. Domb and J.L. Lebowitz (Academic Press, New York, 1983), Vol. 8, p. 269.

[2] A. Billoire, Nucl. Phys. B, Proc. Suppl. **42**, 21 (1995); W. Janke, in *Computer Simulations in Condensed Matter Physics VII*, edited by D.P. Landau, K.K. Mon, and H.B. Schüttler (Springer-Verlag, Heidelberg, 1994), p. 29, and references therein.

[3] B.M. McCoy and T.T. Wu, *The Two-Dimensional Ising Model* (Harvard University Press, Cambridge, MA, 1973); C. Itzykson and J.-M. Drouffe, *Statistical Field Theory* (Cambridge University Press, Cambridge, England, 1989), Vol. I.

[4] F. Y. Wu, Rev. Mod. Phys. **54**, 235 (1982); **55**, 315(E) (1983).

[5] E. Buffenoir and S. Wallon, J. Phys. A **26**, 3045 (1993).

[6] A. Klümper, Int. J. Mod. Phys. B **4**, 871 (1990); A. Klümper, A. Schadschneider, and J. Zittartz, Z. Phys. B **76**, 247 (1989).

[7] C. Borgs and W. Janke, J. Phys. (France) I **2**, 2011 (1992).

[8] P. Peczak and D. P. Landau, Phys. Rev. B **39**, 11 932 (1989).

[9] L. A. Fernandez, J. J. Ruiz-Lorenzo, M. P. Lombardo, and A. Tarancón, Phys. Lett. B **277**, 485 (1992).

[10] S. Gupta and A. Irbäck, Phys. Lett. B **286**, 112 (1992).

[11] W. Janke and S. Kappler, Phys. Lett. A **197**, 227 (1995); Nucl. Phys. B, Proc. Suppl. **34**, 674 (1994).

[12] W. Janke and S. Kappler, Europhys. Lett. **31**, 345 (1995); Nucl. Phys. B, Proc. Suppl. **42**, 770 (1995).
[13] C. Borgs and J. T. Chayes, J. Stat. Phys. **82**, 1235 (1996).
[14] P. W. Kasteleyn and C. M. Fortuin, J. Phys. Soc. Jpn. (Suppl.) **26**, 11 (1969); C. M. Fortuin and P. W. Kasteleyn, Physica (Ultrecht) **57**, 536 (1972); C. M. Fortuin, *ibid.* **58**, 393 (1972); **59**, 545 (1972).
[15] U. Wolff, Phys. Rev. Lett. **62**, 361 (1989).
[16] R. H. Swendsen and J. S. Wang, Phys. Rev. Lett. **58**, 86 (1987).
[17] A. D. Sokal, *Monte Carlo Methods in Statistical Mechanics: Foundations and New Algorithms*, Cours de Troisième Cycle de la Physique en Suisse Romande, Lausanne, 1989; and in *Quantum Fields on the Computer*, edited by M. Creutz (World Scientific, Singapore, 1992), p. 211.
[18] R. G. Miller, Biometrika **61**, 1 (1974); B. Efron, *The Jackknife, the Bootstrap and other Resampling Plans* (SIAM, Philadelphia, PA, 1982).
[19] W. Janke and S. Kappler, J. Phys. (France) I **7**, 663 (1997).
[20] R. J. Baxter, J. Phys. C **6**, L445 (1973); J. Stat. Phys. **9**, 145 (1973).
[21] T. Bhattacharya, R. Lacaze, and A. Morel, Europhys. Lett. **23**, 547 (1993); Nucl. Phys. B, Proc. Suppl. **34**, 671 (1994); Nucl. Phys. B **435**, 526 (1995); Nucl. Phys. B, Proc. Suppl. **42**, 743 (1995); J. Phys. (France) I **7**, 81 (1997).
[22] W. Janke and S. Kappler (unpublished).